ADVANCED ENERGY & SUSTAINABILITY RESEARCH
Open Access
www.advenergysustres.com

Stabilization of ZnO Catalysts for Polyesters Hydrolytic Depolymerization by Incorporation into ZrO_2 Lattice: A Polylactic Acid Case Study

Francesca Liguori, Werner Oberhauser, Enrico Berretti, Lorenzo Poggini, Pierluigi Barbaro, and Carmen Moreno-Marrodán*

Depolymerization is an effective strategy to achieve circularity in polyesters management. However, most of current technologies require organic solvents, homogeneous catalysts, or harsh reaction conditions, while generating considerable amounts of undesired products. Hydrolysis over heterogeneous ZnO catalyst using neat water has shown to be a sustainable method for selective depolymerization, although limited by the interaction of ZnO with the nascent carboxylic acids monomers produced, which leads to catalyst dissolution and deactivation, hence to poor catalyst reusability. Herein we demonstrated that the use of ZnO–ZrO_2 mixed oxide catalysts is a successful strategy to avoid Zn leaching in solution, while maintaining catalyst activity. The hydrolytic depolymerization of polylactic acid over ZnO–ZrO_2 mixed oxides at 130 °C is investigated as reference reaction, showing that catalysts with up to 10% wt Zn content resulted in complete conversion and 100% selectivity to lactic acid, with negligible Zn leaching over repeated catalyst reuses. The catalysts are characterized by a combination of solid-state techniques, suggesting that ZnO stabilization occurs upon incorporation into the lattice of an inert ZrO_2 phase.

1. Introduction

With more than 70 Mt globally produced per year,[1,2] polyesters are among the most popular synthetic organic polymers due to the multiple uses in the everyday life. Polyesters are plastic materials prominent in the textile (≈65%), food packaging, and beverage bottles sectors (≈30%).[3,4] Unfortunately, most polyesters are hardly biodegradable, hence they may accumulate in the environment if not recovered and processed.[5,6] As a consequence of clothes washing, it is estimated that polyesters are the main responsible for microplastics pollution of oceans.[7,8] To date, around 18% of polyesters are mechanically recycled, 25% are incinerated and 54% are landfilled or dispersed.[9,10] Despite poorly developed, chemical recycling, defined by Plastic Europe as the "conversion of polymeric waste by changing its chemical structure to produce substances that are used as products or as raw materials for the manufacturing of products",[11] is the more attractive and promising strategy to implement a true circular economy for plastics.[12,13] Monomers resulting from the depolymerization of polyester scraps or post-consumer goods via chemical recycling are useful building blocks for the production of virgin polymers, dyes, pharmaceuticals, solvents, or food additives.[14,15] However, chemical recycling of polyesters at large must carefully consider economic and environmental impacts to assess competitiveness with complementary recycling options or the replacement of conventional polyesters manufacturing routes.[16,17] Usual strategies for depolymerization of polyesters focus on solvolysis (hydrolysis, alcoholysis, glycolysis, and aminolysis) or hydrogenolysis reactions,[18,19] or the combination of the two.[20,21] Still, few industrial processes are in place requiring harsh reaction conditions and the treatment of considerable amount of waste.[22,23] Use of a catalyst may significantly improve the kinetic, energy inputs, and selectivity of depolymerization, although currently limited to soluble metal salts or strong acidic/basic promoters (KOH, NaOH, H_2SO_4).[24,25] At the industrial level, heterogenous catalysts are preferred due to the ease of recovery, reuse, integration into existing reactor equipment, and product purification, albeit limitations may arise in terms of catalyst durability and leaching of metal species.[26] Therefore, innovative heterogeneous catalytic systems fulfilling sustainability criteria are actively sought.[27,28] In the case of solvolytic depolymerizations, one further drawback stems from the insolubility of polymers in common solvents, which results in the restricted accessibility of polymer chain linkages to a solid catalyst interface.[29,30] Solvent-free processes are thus being

F. Liguori, W. Oberhauser, E. Berretti, L. Poggini, P. Barbaro, C. Moreno-Marrodán
Istituto di Chimica dei Composti Organo Metallici
Consiglio Nazionale delle Ricerche
Via Madonna del Piano 10, 50019 Sesto Fiorentino, Firenze, Italy
E-mail: pierluigi.barbaro@iccom.cnr.it

L. Poggini
Department of Chemistry "U. Schiff"-DICUS- and INSTM Research Unit
University of Florence
Via della Lastruccia 3-13, 50019 Sesto Fiorentino, Italy

The ORCID identification number(s) for the author(s) of this article can be found under https://doi.org/10.1002/aesr.202400349.

DOI: 10.1002/aesr.202400349

developed, although involving high-reaction temperatures above the melting point of the polymers.[31,32]

We previously described the hydrolytic depolymerization reaction of polylactic acid (PLA) and polyethylene terephthalate (PET) over insoluble ZnO catalyst to yield lactic acid (LA), ethylene glycol (EG), and terephthalic acid (TPA) monomers, respectively.[33] Benefits of the method include: use of neat water as the only reagent, no need for soluble additives, promoters or co-solvents, reaction temperature well below the melting point of the polymers, faster kinetic compared to the catalyst-free process, >98% selectivity to monomers at full polyester conversion, no salt by-products, inexpensive catalyst. ZnO showed a catalytic activity superior to that of other insoluble metal oxides. Drawback of the method is the decrease of activity observed upon catalyst recycling, which is attributed to the formation of Zn species having lower or no catalytic activity, and resulting from the interaction of amphoteric ZnO with the nascent carboxylic acids monomers. In the case of PLA hydrolysis, these species are water-soluble, which results in Zn loss in solution, hence to partial ZnO recovery.

Aiming at the development of stable and reusable heterogeneous hydrolytic depolymerization catalysts, herein we report a strategy for the stabilization of ZnO, based on the incorporation of the ZnO active sites into a ZrO_2 solid lattice. Mixed ZnO–ZrO_2 oxides were prepared and tested in the hydrolysis reaction of PLA and scrutinized for efficiency, stability and reusability. An accurate analysis of Zn and Zr leaching in solution was performed upon change of catalyst composition and reaction conditions.

The market PLA is considerably increasing in view of the substitution of oil-derived PET in food packaging and in single-use product applications,[34,35] as well as for its compostability. However, because of the slow degradation of PLA in the environment and the need for specialized microorganisms,[36,37] biodegradation of PLA cannot be considered an actual recycling option, rather a chance for the management of its uncontrolled waste streams. In addition, biodegradation of PLA does not produce reusable monomers, but mainly CO_2,[38] therefore methods for the chemical depolymerization of PLA are of current industrial interest.[39,40] Besides these considerations, the hydrolysis of PLA was chosen as test reaction because, compared to other polyesters, the LA formed is a water-soluble, high strength acid provided with by notable chelating properties,[41,42] hence more reactive toward ZnO. LA is a valuable platform molecule for a variety of chemicals, with a current demand around 400 ktons $year^{-1}$.[43]

Mixed ZnO–ZrO_2 oxides with various Zn content (up to 95% mol) have been reported in the literature as catalysts for the gas-phase alkane dehydrogenation[44] and CO_2 reduction reactions,[45,46] and the hydrothermal degradation of cotton cellulose (190 °C).[47] No applications are known for treatment and depolymerization of plastics.

2. Results and Discussion

2.1. Catalysts Synthesis

A series of ZnO–ZrO_2 mixed oxides with different Zn content were synthesized and preliminary characterized by Inductively coupled plasma optical emission spectroscopy (ICP-OES), for Zn quantification, and nitrogen sorption, for morphological analysis of the solid materials. A summary of the corresponding data is reported in **Table 1** and in Table S1, Supporting Information together with the labeling scheme adopted. ZnO–ZrO_2–20 and ZnO–ZrO_2–10 labels represent the higher and the lower Zn content in the catalysts, respectively.

The catalysts were prepared by one-pot co-precipitation, by weighting appropriate amounts of $ZrO(NO_3)_2$ and $Zn(NO_3)_2$ precursors in the presence of $(NH_4)_2CO_3$ in water, followed by solvent evaporation, washing, and calcination at 500 °C.[48] Both ZnO–ZrO_2–10 and ZnO–ZrO_2–20 oxides resulted in a mixture of Type II (non-porous) and Type IV (mesoporous) isotherm, with a type H3 hysteresis loop associated to 22.6 and 5.9 nm size mesopores, for ZnO–ZrO_2–10 and ZnO–ZrO_2–20, respectively, and low BET surface areas of 5.34 and 27.89 $m^2\ g^{-1}$, respectively (Figure S2 and S3, Supporting Information). ZnO–ZrO_2–20 also exhibited a nearly horizontal and parallel Type H4 hysteresis loop over a wide range of p/p°.

2.2. Catalytic Reactions

In a preliminary set of experiments, the ZnO–ZrO_2 mixed oxides were tested as catalysts in the hydrolytic depolymerization reaction of PLA, and compared with the catalyst-free run under identical reaction conditions, that is, using the same Zn quantity (0.06 mmol, based on catalyst composition), polyester and water amounts, reaction temperature and time (24 h). A reaction temperature of 130 °C was adopted as reference value.[33] Representative results are reported in graphical format in **Figure 1**. Compared to the blank experiment, pure ZrO_2 oxide did not improve PLA hydrolysis. By contrast, ZnO-containing oxides resulted in significantly higher LA yields, which decreased in the order ZnO > ZnO–ZrO_2–20 > ZnO–ZrO_2–10. While these results confirm that ZnO is the catalytically active species, the trend observed is ascribable to an effect of the ZrO_2 environment onto the active sites, and not to the overall catalysts porosity or granulometry (≈100 µm), which are very similar anyway (see above), and do not justify for the observed yields (Table 1). Interestingly, Zn leaching in solution upon use of mixed oxide catalysis is observed, whose amount % is much lower for the ZnO–ZrO_2–10 catalyst, than for the other oxides (Table S2, Supporting Information). The contribution of soluble Zn species to the conversion of PLA could be ruled out by the lack of catalytic activity shown by the aqueous mixture recovered after

Table 1. Composition and porosity of ZnO–ZrO_2 mixed oxides.[a)]

Label	Zn [% wt][b)]	V [$cm^3\ g^{-1}$]	D [nm]	S [$m^2\ g^{-1}$]
ZnO[c)]	80.3 ± 6.0	0.024	11.8	7.11
ZrO_2	–	0.054	5.0	29.26
ZnO–ZrO_2–10	7.3 ± 2.0	0.028	22.6	5.34
ZnO–ZrO_2–20	14.3 ± 4.3	0.054	5.9	27.89

[a)]BJH desorption cumulative pore volume (V) and desorption average pore diameter (D), BET surface area (S). [b)]Bulk Zn content. Data from ICP-OES analysis. Mean values over three samples. [c)]Data from ref. [33].

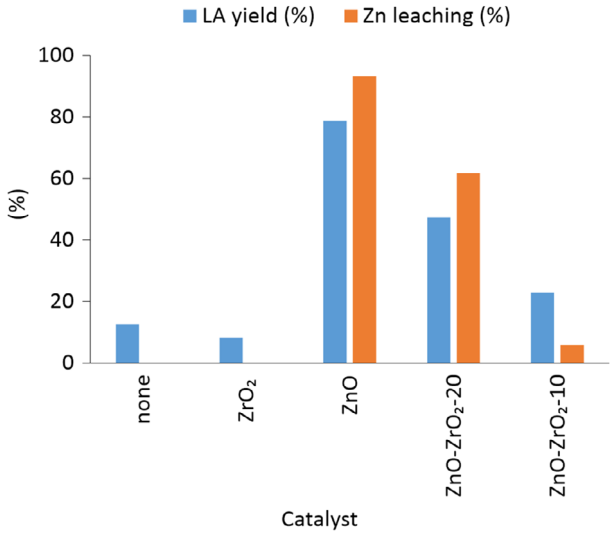

Figure 1. Selected data for the normalized hydrolysis reaction of PLA over solid ZnO–ZrO_2 catalysts. Reaction conditions: 0.06 mmol Zn loading, 0.28 mmol PLA, 10 mL water, 130 °C, 24 h reaction time (ZrO_2 and ZnO–ZrO_2–10 catalyst 52 mg, ZnO 5.1 mg, ZnO–ZrO_2–20 29 mg). LA yield from HPLC analysis, based on number of PLA repetition units. Data for Zn leaching (% of Zn used) from ICP-OES analysis of the recovered reaction solutions.

catalysis.[33,49] Under the reaction conditions adopted, no oligomers or products other than LA were observed by HPLC, ^{1}H-NMR, GC-MS, and GPC analysis. Appropriate choice of reaction conditions allowed 100% LA yield for all catalysts examined (e.g. 72 h reaction time). The powder X-ray diffraction (PXRD) spectra of the solid oxides recovered after use in catalysis were identical to that of the starting catalysts used (*vide infra*).

Prompted by the aforementioned findings, we focused on ascertaining the stabilization effect of the ZrO_2 lattice onto the ZnO active sites. Previous reports indicate the mechanism of ZnO-catalyzed hydrolysis of polyesters to occur via Lewis-acid Zn^{2+} activation of the carbonyl ester bond chain linkages, which undergo nucleophile attack by water, leading to depolymerization.[50,51] Zn leaching in solution upon catalyst usage is attributable to the interaction of the nascent LA resulting from hydrolysis with amphoteric ZnO,[33] to generate soluble,[52] yet under our reaction conditions catalytically inactive, "zinc-lactate" species (**Figure 2**).[53,54] Assuming the reaction stoichiometry, it is expected that for pure ZnO complete Zn leaching and ZnO loss in solution is observed once the value of "LA formed/ZnO used" molar ratio is greater than two. A second set of experiments, carried out at increasing reaction time and monitoring LA yield with respect to ZnO used, were consistent with this hypothesis, within the experimental errors. Results are graphically reported in **Figure 3**, red line, and in Table S3 and Figure S8, Supporting Information. A perusal of the hydrolysis results showed the ZrO_2 lattice to have no or little stabilization effect on the ZnO sites in the mixed oxide ZnO–ZrO_2–20 catalyst, since the % of Zn leached in solution was just below that of pure ZnO over the whole range of LA amount produced (Figure 3, blue line). By contrast, the ZnO–ZrO_2–10 catalyst with low Zn content showed to be considerably more stable under the reaction

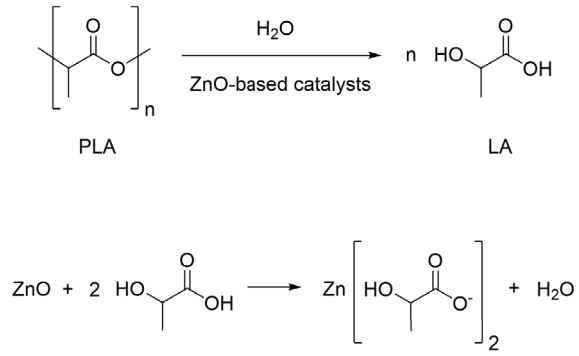

Figure 2. Schematic representation of the ZnO-catalyzed hydrolysis reaction of PLA (top) and lactate species formation (bottom).

conditions adopted. In that case, the amount of Zn leached in solution at full PLA conversion (i.e., molar ratio LA formed/ZnO used = 4.5) was ≈8% of the quantity used (Figure 3, green line), which is much less than that found for the other catalysts. In other words, under identical reaction conditions, the ZnO contained in the ZnO–ZrO_2–10 catalyst was converted to only 8% of the maximum obtainable "Zn(lactate)$_2$" specie, whereas the corresponding value for pure ZnO and for ZnO–ZrO_2–20 was 100% and ≈79%, respectively.[48]

To further substantiate our hypothesis, we performed a catalyst stability test under hydrolytic depolymerization reaction conditions, that is, by contacting the mixed oxide catalysts with a 4.5-fold molar excess LA/Zn, under 130 °C and 24 h. The amount of Zn leached in solution was 4.5%, 79.3%, and 94.8% (wt) of that used in catalysts, for ZnO–ZrO_2–10, ZnO–ZrO_2–20 and for pure ZnO, respectively, which confirms the substantial

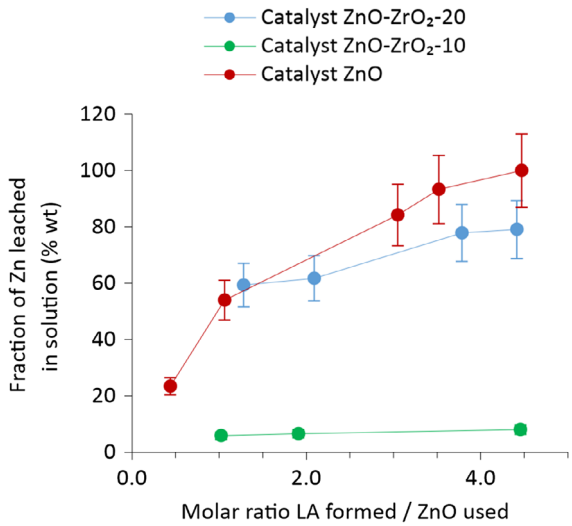

Figure 3. Leaching of Zn versus ratio of [LA formed/ZnO used] for the hydrolysis reaction of PLA over solid ZnO–ZrO_2 catalysts. Reaction conditions: molar ratio [PLA/ZnO used] = 4.5 based on number of PLA repetition units and ZnO content in the mixed oxide solid catalysts, 10 mL water, 130 °C, 17–72 h reaction time. LA yield from HPLC analysis. Data for Zn leaching in solution from ICP-OES analysis.

inhibition of the reaction between LA and ZnO in the ZnO–ZrO_2–10 mixed-oxide (Table S4, Supporting Information).

Having established that ZnO–ZrO_2–10 is an effective and comparatively stable catalyst for the hydrolytic depolymerization reaction of PLA, we examined its potential for recovery and reuse by performing a series of catalyst recycling experiments. After use in PLA hydrolysis, the solid catalyst was recovered by centrifugation, weighted, and reused in a next hydrolysis experiment under identical reaction conditions. Representative results are reported in **Figure 4**. No significant activity decay was observed over three catalytic cycles, where an average 99% LA yield (HPLC) and 33 ppm Zn leaching in solution (ICP-OES) were obtained for each 72 h reaction time runs (Table S5, Supporting Information). Ion-exchange resin filtration of the reaction solution recovered after each cycle enabled 99% removal of soluble Zn species.[33] Under the same reaction conditions, the catalyst-free experiment gave LA in 27% yield.

Compared to the catalyst-free system, the effect of accelerating the kinetic of hydrolytic depolymerization reaction using the ZnO–ZrO_2–10 catalyst is highlighted in **Figure 5**, where LA yields *versus* reaction time are reported for both systems. Under identical reaction conditions (130 °C, 72 h), LA yield was 27% and >99% for the un-catalyzed and catalyzed hydrolysis reaction, respectively, corresponding to a productivity of 3.75×10^{-3} and 13.75×10^{-3} ($mol_{LA}\ mol_{PLA}^{-1}\ h^{-1}$) in the two cases.

The hydrolytic depolymerization of PLA to LA by chemical catalysts was previously described in the literature using soluble acid/base promoters.[55,56] On the industrial scale, NatureWorks recycles PLA wastes into LA by nitric acid-mediated hydrolysis,[57] whereas the LOOPLA process provides mixtures of LA and lactate esters by treatment of PLA with an excess of aqueous NaOH at 90 °C or with ethyl lactate at 140 °C.[58] To the best of our knowledge, with the exception of pure ZnO,[33] no heterogeneous catalysts have been described for the complete and selective

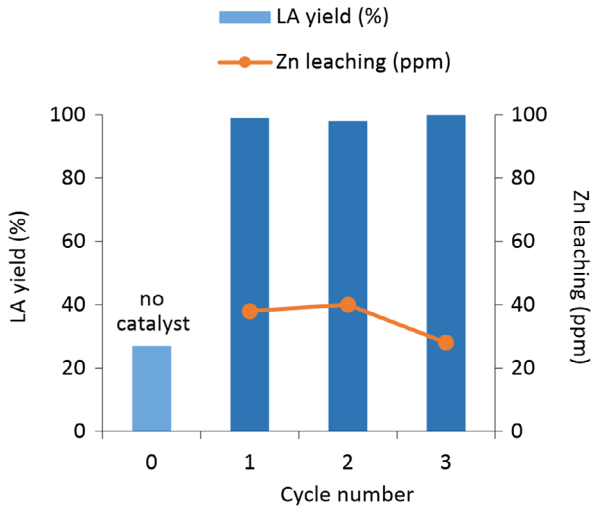

Figure 4. Recycling of ZnO–ZrO_2–10 catalysts in the hydrolysis reaction of PLA. Reaction conditions: 0.28 mmol PLA, 52 mg catalyst (starting, corresponding to 0.06 mmol Zn), 10 mL water, 130 °C, 72 h reaction time. LA yield data (left) from HPLC analysis, based on number of PLA repetition units. Zn leaching (right) from ICP-OES analysis of the recovered reaction solution.

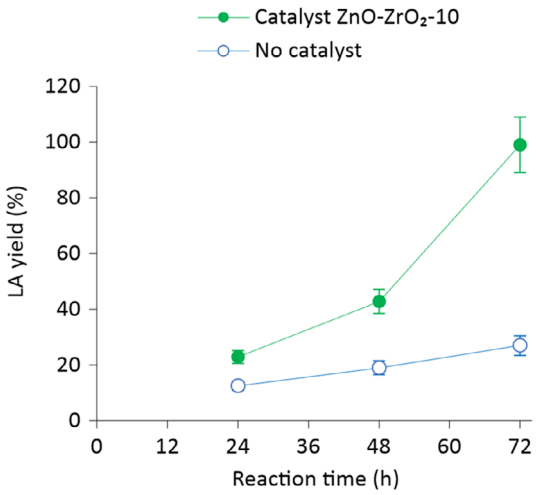

Figure 5. Hydrolytic depolymerization of PLA in neat water without and with heterogeneous ZnO–ZrO_2–10 catalyst. Reaction conditions: 10 mL water, 130 °C, 0.28 mmol PLA, 52 mg catalyst, 0.06 mmol Zn. Yield from HPLC analysis, based on number of PLA repetition units.

depolymerization reaction of PLA to LA monomer in neat water. The depolymerization of PLA was recently reported over solid-supported Ru@CeO_2 catalyst. The system requires 200 °C, 100 bar H_2 and H_2O to give LA in 95% selectivity at 98% PLA conversion.[59] Role of Ru metal is unclear, whereas the catalyst showed a drastic decrease of efficiency upon reuse. PLA/ZnO nanocomposites were described to undergo hydrolytic degradation either in water or in phosphate buffered and NaOH solutions.[60,61]

ZnO has been used as catalyst in a variety of applications.[62,63] Depolymerization of plastics include hydrolysis, aminolysis, and alcoholysis of polycarbonates using a ZnO/tetrabutylammonium chloride ionic liquid system in THF solution,[64] and the alcoholysis and glycolysis reactions of PET.[65] In the case of PET methanolysis to give dimethylterephthalate, a dispersion of 4 nm ZnO nanoparticles performed as pseudo-homogeneous catalyst, however with ≈30% activity decrease upon reuse at 170 °C.[66] In the case of PET glycolysis to yield bis(2-hydroxyethyl)terephthalate (BHET) at 300 °C, the catalyst consisted in ZnO nanoparticles deposited onto preformed 60 nm silica spheres.[67,68] No information on catalyst stability was available, however. 2% mol Ag-doped ZnO nanoparticles were used as catalyst for the glycolysis reaction of PET textile wastes under microwave irradiation at 200 °C.[69] Other works describe the use of insoluble catalysts (SnO, Sb_2O_3) for the conversion of PLA to lactide (3,6-Dimethyl-1,4-dioxan-2,5-dione).[70]

2.3. Catalysts Characterization

The oxide catalysts were characterized in the solid state by a combination of microscopy, diffraction, and spectroscopic techniques.

The PXRD spectrum of pure ZrO_2 (**Figure 6**, trace a) revealed the presence of a mixture of monoclinic (P121/c1) and tetragonal phases (P42/nmc).[71] By contrast, the PXRD spectra of the mixed

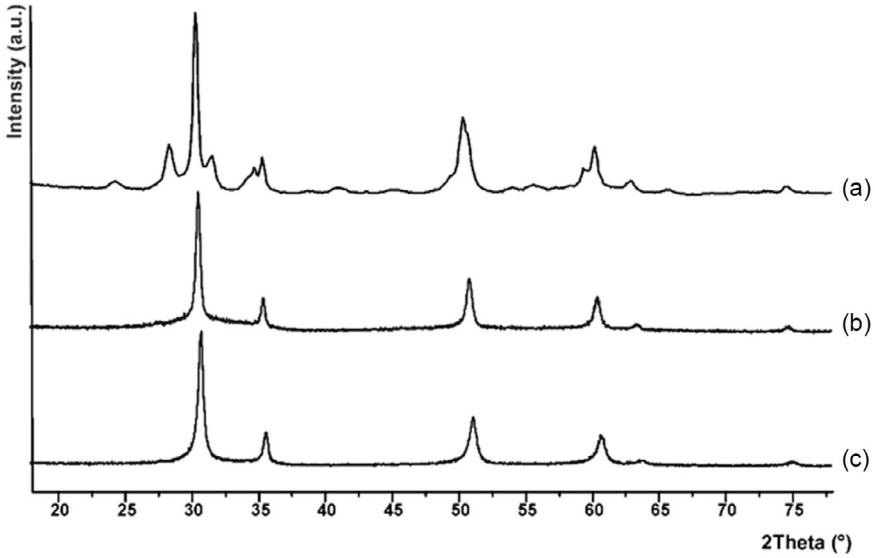

Figure 6. PXRD spectra acquired at room temperature for: a) ZrO_2, b) ZnO–ZrO_2–10, and c) ZnO–ZrO_2–20.

ZnO–ZrO_2 oxides showed a crystalline ZrO_2 tetragonal phase only, and no crystalline ZnO phase could be detected. In addition, compared to pure ZrO_2, the spectrum of ZnO–ZrO_2–10 showed a 0.2° shift to higher 2θ value for the 011 Bragg reflex of the tetragonal phase centered at 30.42° (2θ) (Figure 6, trace b). This finding indicates the partial exchange of Zr^{4+} by Zn^{2+} in the lattice of ZrO_2, thus leading to a shrinking of the crystal lattice of ZrO_2, because of the smaller ionic radius of Zn^{2+} (74 Å) with respect to Zr^{4+} (84 Å).[72,73] A further shift of the 011 Bragg reflex to 30.61° (2θ), along with a broadening of the Bragg reflexes, was visible in the spectrum of ZnO–ZrO_2–20 (Figure 6, trace c), confirming that the replacement of Zr by Zn ions is going further in this latter oxide. The determination of the crystallite size by means of the Debye–Scherrer method,[74] and referring to the 011 Bragg reflex centered at ≈30.0 (θ), gave a crystallite size of 36.1 and 28.1 nm for ZnO–ZrO_2–10 and ZnO–ZrO_2–20, respectively, which is in line with the crystallite size obtained for related mixed ZnO–ZrO_2 phases.[75] Pure ZnO shows a hexagonal phase.[33]

A variable-temperature PXRD study was performed on the crude synthetic reaction mixture of ZnO–ZrO_2–10 after water evaporation, showing the sample to contain a crystalline $(NH_4)NO_3$ phase,[76] and an amorphous phase build up by $Zr(OH)_4$ and $Zn(OH)_2$ (Figure S4, Supporting Information trace a).[77] Upon washing with water followed by drying, $(NH_4)NO_3$ was completely removed (Figure S4, Supporting Information trace b). The amorphous phase was heated under air in a heating chamber from room temperature to 500 °C, and XRD spectra were acquired at different temperatures (Figure S4, Supporting Information traces c–f). The formation of the crystalline tetragonal ZrO_2 phase was observed at 450 °C, and the final crystallinity of ZrO_2 obtained after 3 h at 500 °C corresponded to that obtained by the muffle furnace heating.

Low-magnification transmission electron microscopy (TEM) investigations showed the sonicated mixed oxide samples to consist in aggregates of ≈100–200 nm size (**Figure 7**). High-magnification HR-TEM experiments highlighted the presence of ordered crystallographic entities in the 10–40 nm

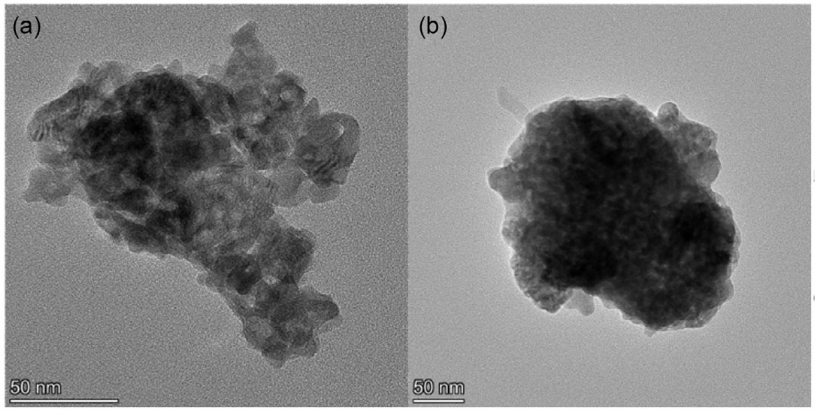

Figure 7. Low-magnification TEM images of sonicated mixed oxide samples: a) ZnO–ZrO_2–10, and b) ZnO–ZrO_2–20.

dimensional range, whose fringes could be ascribed mainly to the monoclinic structure of ZrO_2. These ordered entities appear to be continuous in the bulk of the particles. Only few peripheral spots showed presence of an amorphous matrix which seemed to intercalate the crystalline entities (**Figure 8**c). No fringes attributable solely to ZnO were visible for both the ZnO–ZrO_2–10 and ZnO–ZrO_2–20 samples, as illustrated in Figure 8.

The homogeneous composition of the materials was also confirmed by energy dispersive X-ray spectroscopy (EDX) mapping, performed on both the mixed oxides. Uniform bulk distribution of Zn and Zr was noticeable along the sampled particles (both in the crystalline and amorphous phases), whose compositional results were in line with the bulk quantification obtained from ICP-OES analysis (Table S1, Supporting Information). Representative images are reported in **Figure 9** and in Figure S5, Supporting Information for the ZnO–ZrO_2–10 and ZnO–ZrO_2–20 catalysts, respectively. This composition trend was confirmed by line profile analyses performed on different particles (Figure S6, Supporting Information as example).

X-ray photoelectron spectroscopy measurements (XPS) were carried out on the mixed oxides to define the oxidation state of the species involved. Compared to pure ZnO (1020.8 eV),[78] the Zn 2*p* region of both ZnO–ZrO_2–10 and ZnO–ZrO_2–20 was shifted to higher binding energy by 1.6 eV (**Table 2**), suggesting a similar chemical environment in the two cases. The region was composed by the usual Zn 2*p* doublets (Figure S7, Supporting Information green filling), plus a minor peak at lower binding energy ascribable to impurities (Figure S7, Supporting Information blue filling),[79] and the O^{KLL} Auger peak at ≈1040 eV. Concerning the Zr region, there are no appreciable differences between pure ZrO_2 and the ZnO–ZrO_2–20 and ZnO–ZrO_2–10 oxides.[80] The Zr 3*d* region is characterized by the presence of a component at ≈182.4 eV, as expected from the literature. The shift observed in the Zn 2*p* region can be attributed to a transfer of electron density from Zn^{2+} to the neighboring O^{2-}.[44] The surface composition of the oxide catalysts was estimated by XPS (Table S1, Supporting Information), and compared to the bulk composition obtained from ICP-OES and EDX analysis, indicating a Zn-richer surface in the case of ZnO–ZrO_2–20 (see next Section).

2.4. Catalysts Performance Comparison

Co-precipitated mixed zinc–zirconium oxides have been reported and characterized in the literature, showing Zn^{2+} to form solid solutions with zirconia within certain limits. The upper concentration limit of Zn in the ZrO_2 matrix was indicated to be around 25% molar fraction.[81] In the case in our hands, mixed oxides were prepared with different Zn bulk content (Table S1, Supporting Information), whereby Zn is mostly embedded in the ZrO_2 lattice (see above PXRD, HRTEM, ICP-OES and XPS characterization). ICP-OES analysis indicated a 15.8% Zn molar fraction bulk composition for the ZnO–ZrO_2–10 oxide (Zn/(Zn+Zr) mol), whilst the value for the higher-Zn content ZnO–ZrO_2–20 oxide was 27.4%, that is, slightly above the Zn

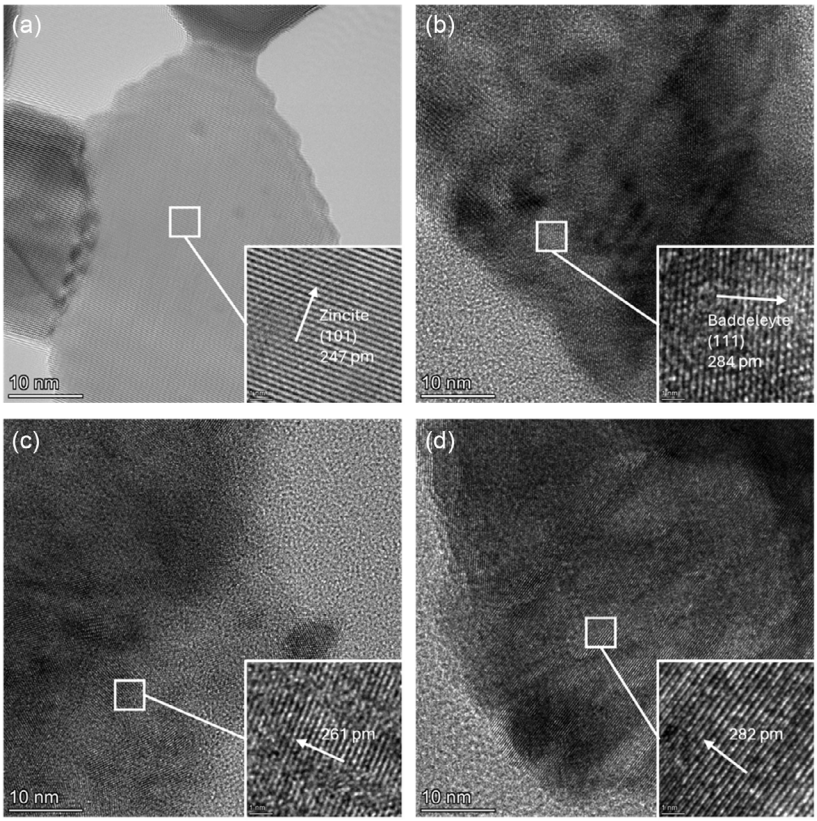

Figure 8. HR-TEM images of: a) ZnO, b) ZrO_2, c) ZnO–ZrO_2–10, d) ZnO–ZrO_2–20. The spacings shown in c) and d) are associable to ZrO_2 structure.

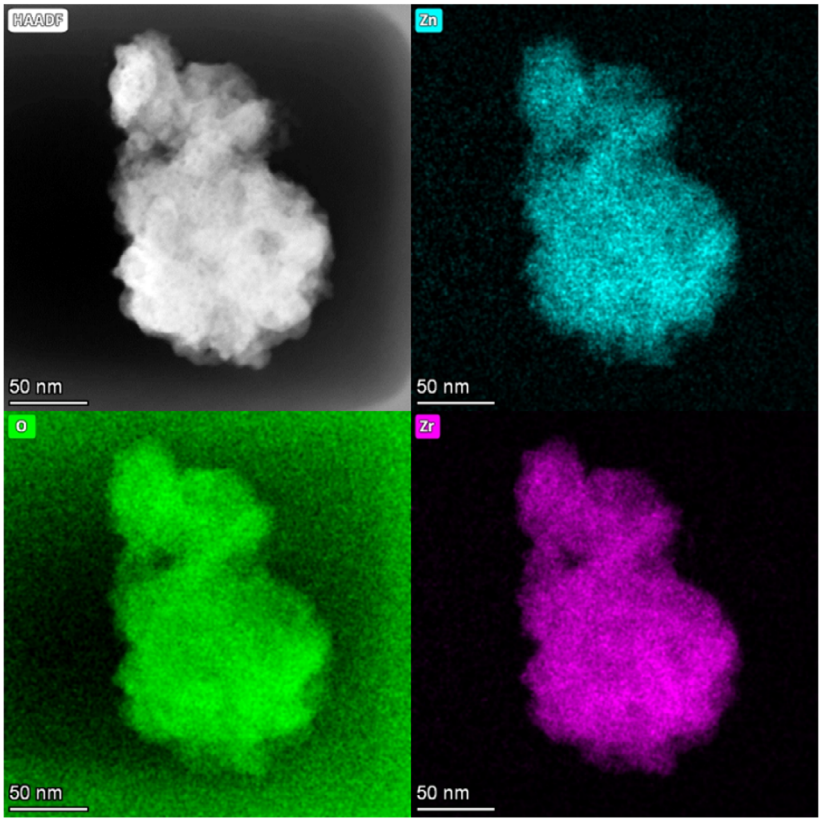

Figure 9. High-angle annular dark-field image (HAADF, top left) and zinc (cyano), oxygen (green) and zirconium (purple) EDX maps of ZnO–ZrO_2–10 oxide.

Table 2. Selected XPS binding energy data for ZnO–ZrO_2 mixed oxides.

Label	Binding energy [eV]		References
	Zn $2p_{3/2}$	Zr $3d_{5/2}$	
ZnO	1020.8	–	[78]
ZrO_2	–	182.5	[80]
ZnO–ZrO_2–10	1022.4	182.4	This work
ZnO–ZrO_2–20	1022.4	182.3	This work

solubility limit. The bulk (ICP) and surface (XPS) composition of the two mixed oxides is reported in graphical format in **Figure 10**. For the ZnO–ZrO_2–20 sample, XPS analysis suggested this Zn^{2+} "surplus" to arrange on the surface of the mixed oxide, thus resulting in a Zn-richer surface (32% Zn molar fraction), compared to the bulk phase. The different bulk-to-surface composition is clearly visible in Figure 10. By contrast, for ZnO–ZrO_2–10 surface and bulk compositions were comparable within the experimental errors. A similar preferred surface arrangement was previously described for other Zn–Zr mixed oxides having comparable Zn loading.[45,82]

On the above basis, we can argue that the different catalytic performance of the mixed oxides synthesized is attributable to the different Zn distribution in the materials. That is, the ZnO–ZrO_2–20 catalyst, featuring a higher density of surface-exposed

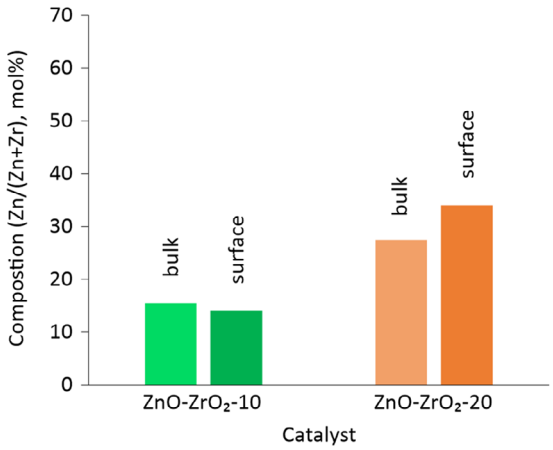

Figure 10. Bulk and surface composition (Zn molar fraction %) of the ZnO–ZrO_2–10 and ZnO–ZrO_2–20 oxides, as obtained from ICP-OES and XPS analysis, respectively.

Zn species, is provided with a better site-accessibility, which results in both an enhanced Lewis-acid activation of ester bonds, hence in a higher catalytic activity for depolymerization, on one hand, and in an easier interaction with the nascent LA formed upon hydrolysis, hence in a greater Zn leaching in solution on the other hand. In other words, stabilization of the ZnO–ZrO_2–10 catalyst having a lower Zn content occurs via

"entrapment" of most Zn^{2+} into the bulk ZrO_2 lattice, which hampers Zn^{2+} interaction and complexation by LA, hence prevents ZnO dissolution in acidic media. Figure S9, Supporting Information reports the relationship between catalytic performance (productivity and stability) and surface composition for the tested catalysts. An analogous activity-enhancement behavior in surface-enriched mixed ZnO–ZrO_2 oxide catalysts was previously suggested for the hydrogenation reaction of CO_2 to methanol.[75,82]

3. Conclusions

Selective depolymerization by chemical recycling is an effective approach to achieve circularity of polyester materials. However, current technologies mostly rely on homogeneous catalysts, considerable amounts of soluble acid-base promoters, harsh reaction conditions, toxic reagents or complex separation-purification procedures, which ultimately result in environmentally and economically non-competitive processes, compared to other conventional recycling options. Solvolysis in neat water represent a greener alternative, provided that suitable heterogeneous catalysts are developed. To this aim, ZnO has shown to be highly efficient, although reaction with nascent carboxylic acids to obtain soluble, yet catalytically inactive species, limits its applicability. Typical is the case of PLA hydrolysis, which results in the quantitative formation of "Zn-lactate" compounds, hence in substantial catalyst loss. Herein we reported a detailed investigation of the catalytic performance of mixed ZnO–ZrO_2 oxides toward PLA hydrolysis, including quantification and mechanism for metal leaching. We unequivocally demonstrated that the use of inexpensive, heterogeneous ZnO–ZrO_2 oxide catalysts, with up to 10% wt Zn content, results in the hydrolytic depolymerization of PLA to be achieved with negligible Zn leaching under mild reaction conditions (130 °C), and with 100% selectivity at full PLA conversion. The mixed oxide catalyst can be quantitatively recovered by simple centrifugation and reused with no detectable performance decay, hence significantly contributing to the overall catalyst productivity. The stabilization of the ZnO catalytically active species can be attributed to their embedding into the bulk lattice of inert ZrO_2.

Research in advanced catalytic methods for plastics depolymerization are currently pursued, particularly targeting heterogeneous catalyst, in the perspective of implementing more sustainable recycling processes.[83,84] Common issues in the field relate to catalyst cost, activity, stability and reusability. The findings herein illustrated may be helpful to this purpose, by offering new insights into the degradation of effective ZnO-based catalysts and a design strategy for catalysts with improved resistance toward hydrolysis, potentially usable with other polymeric materials (polyamides, polyurethanes, polycarbonates) and lytic agents (alcohols, glycols, amines), thus to assist the ambitious circular economy goals for plastics.[85]

Supporting Information

Supporting Information is available from the Wiley Online Library or from the author.

Acknowledgements

Thanks are due to the Made in Italy – Circular and Sustainable (MICS) Extended Partnership, funded by the European Union Next-Generation EU (Piano Nazionale di Ripresa e Resilienza (PNRR) – Missione 4, Componente 2, Investimento 1.3 – D.D. 1551.11-10-2022, PE00000004); the LABSolve "Lactic Acid Based new green Solvents: design, synthesis and use in catalysis" project (20229P7PPM) funded by PNRR, Missione 4 "Istruzione e Ricerca" – Componente C2 Investimento 1.1, "Fondo per il Programma Nazionale di Ricerca e Progetti di Rilevante Interesse Nazionale (PRIN); and to the "Le materie prime del futuro da fonti non-critiche, residuali e rinnovabili" (FutuRaw) project, Fondo Ordinario Enti di Ricerca (D.M. 789, 2023), Ministero dell'Università e della Ricerca, Italia, for financial support. Thanks are also due to Carlo Bartoli (ICCOM-CNR) for reactor design; Fabio Migliacci (ICCOM-CNR) for technical assistance, Elisa Passaglia (ICCOM-CNR) for GPC measurements; Brunetto Cortigiani (University of Florence) for assistance in using the MatchLab platform and to Dr. Filippo Bossola (SCTITEC-CNR) for helpful discussion.

Conflict of Interest

The authors declare no conflict of interest.

Author Contributions

Francesca Liguori: formal analysis (equal); investigation (lead); validation (equal). **Werner Oberhauser**: formal analysis (equal); investigation (equal). **Enrico Berretti**: formal analysis (equal); investigation (equal). **Lorenzo Poggini**: formal analysis (equal); investigation (equal). **Pierluigi Barbaro**: funding acquisition (lead); supervision (lead); writing—original draft (lead). **Carmen Moreno-Marrodán**: validation (equal); visualization (lead).

Data Availability Statement

The data that support the findings of this study are available in the supplementary material of this article.

Keywords

depolymerization, heterogeneous catalysis, hydrolysis, polyester, zinc oxide

Received: October 21, 2024
Revised: November 29, 2024
Published online:

[1] Plastics Europe, Association of Plastics Manufacturers, **2022**, https://plasticseurope.org/knowledge-hub/plastics-the-facts-2022 (accessed: May 2024).
[2] Textile Exchange, **2023**, https://textileexchange.org/knowledge-center/reports/materials-market-report-2023/ (accessed: May 2024).
[3] M. Rabnawaz, I. Wyman, R. Auras, S. Cheng, *Green Chem.* **2017**, *19*, 4737.
[4] Eunomia, **2022**, https://eunomia.eco/reports/pet-market-in-europe-state-of-play-2022/ (accessed: May 2024).
[5] A. K. Urbanek, A. M. Mirończuk, A. García-Martín, A. Saborido, I. de la Mata, M. Arroyo, *BBA-Proteins Proteomics* **2020**, *1868*, 140315.
[6] I. Taniguchi, S. Yoshida, K. Hiraga, K. Miyamoto, Y. Kimura, K. Oda, *ACS Catal.* **2019**, *9*, 4089.

[7] L. Peng, D. Fu, H. Qi, C. Q. Lan, H. Yu, C. Ge, *Sci. Total Environ.* **2020**, *698*, 134254.
[8] European Environment Agency, **2022**, https://www.eea.europa.eu/publications/microplastics-from-textiles-towards-a (accessed: May 2024).
[9] M. W. Ryberg, A. Laurent, M. Hauschild, United Nations Environment Programme, **2018**, https://www.unep.org/resources/report/mapping-global-plastics-value-chain-and-plastics-losses-environment-particular (accessed: May 2024).
[10] http://www.demeto.eu (accessed: May 2024).
[11] Plastics Europe, Association of Plastics Manufacturers, **2022**, https://plasticseurope.org/knowledge-hub/the-circular-economy-for-plastics-a-european-overview-2/ (accessed: April 2024).
[12] European Commission, **2018**, https://eur-lex.europa.eu/legal-content/EN/TXT/?uri=COM:2018:28:FIN (accessed: Decemeber 2024).
[13] G. W. Coates, Y. D. Y. L. Getzler, *Nat. Rev. Mater.* **2020**, *5*, 501.
[14] R. A. Clark, M. P. Shaver, *Chem. Rev.* **2024**, *124*, 2617.
[15] H. Mangold, B. von Vacano, *Macromol. Chem. Phys.* **2022**, *223*, 2100488.
[16] Closed Loop Partners, **2021**, https://www.closedlooppartners.com/appendix-molecular-recycling-technologies/ (accessed: Decemeber 2024).
[17] N. J. Berger, C. Pfeifer, *Biomass Conv. Bioref.* February **2024**.
[18] Y. Weng, C. B. Hong, Y. Zhang, H. Liu, *Green Chem.* **2024**, *26*, 571.
[19] J. Payne, M. D. Jones, *ChemSusChem* **2021**, *14*, 4041.
[20] A. C. Fernandes, *Green Chem.* **2021**, *23*, 7330.
[21] J. Xu, K. Zhou, L. Qin, Z. Tan, S. Huang, P. Duan, S. Kang, *Polymers* **2023**, *15*, 413.
[22] S. Hann, T. Connock, **2020**, https://www.eunomia.co.uk/reports-tools/final-report-chemical-recycling-state-of-play/ (accessed: Decemeber 2024).
[23] Zero Waste Europe, **2020**.
[24] F. Liguori, C. Moreno-Marrodán, P. Barbaro, *Beilstein J. Org. Chem.* **2021**, *17*, 589.
[25] A. B. Raheem, Z. Z. Noor, A. Hassan, M. K. A. Hamid, S. A. Samsudin, A. H. Sabeen, *J. Cleaner Prod.* **2019**, *225*, 1052.
[26] D. J. Cole-Hamilton, R. P. Tooze, in *Catalyst Separation, Recovery and Recycling: Chemistry and Process Design*, Springer, Dordrecht **2006**.
[27] M. Chu, Y. Liu, X. Lou, Q. Zhang, J. Chen, *ACS Catal.* **2022**, *12*, 4659.
[28] L. O. Mark, M. C. Cendejas, I. Hermans, *ChemSusChem* **2020**, *13*, 5808.
[29] B. D. Vogt, K. K. Stokes, S. K. Kumar, *ACS Appl. Polym. Mater.* **2021**, *3*, 4325.
[30] S. Thiyagarajan, E. Maaskant-Reilink, T. A. Ewing, M. K. Julsing, J. van Haveren, *RSC Adv.* **2022**, *12*, 947.
[31] J. Ge, B. Peters, *Chem. Eng. J.* **2023**, *466*, 143251.
[32] X. Bai, D. R. Aireddy, A. Roy, K. Ding, *Angew. Chem., Int. Ed.* **2023**, *62*, e202309949.
[33] F. Liguori, C. Moreno-Marrodán, W. Oberhauser, E. Passaglia, P. Barbaro, *RSC Sustainability* **2023**, *1*, 1394.
[34] K. J. Jem, B. Tan, *Adv. Ind. Eng. Polym. Res.* **2020**, *3*, 60.
[35] K. Masutani, Y. Kimura, in *Poly(Lactic Acid) Science and Technology: Processing, Properties, Additives and Applications* (Eds: A. Jiménez, M. Peltzer, R. Ruseckaite), Royal Society of Chemistry, Cambridge **2015**.
[36] B. Laycock, M. Nikolić, J. M. Colwell, E. Gauthier, P. Halley, S. Bottle, G. George, *Prog. Polym. Sci.* **2017**, *71*, 144.
[37] P. Sangwan, D. Y. Wu, *Macromol. Biosci.* **2008**, *8*, 304.
[38] H. Tsuji, K. Suzuyoshi, *Polim. Degrad. Stab.* **2002**, *75*, 347.
[39] V. Aryan, D. Maga, P. Majgaonkar, R. Hanich, *Resour. Conserv. Recycl.* **2021**, *172*, 105670.
[40] M. C. D'Alterio, I. D'Auria, L. Gaeta, C. Tedesco, S. Brenna, C. Pellecchia, *Macromolecules* **2022**, *55*, 5115.
[41] F. Cariati, F. Morazzoni, G. M. Zanderighi, G. Marcotrigiano, G. C. Pellacani, *Inorg. Chim. Acta* **1977**, *21*, 133.
[42] H. Thun, W. Guns, F. Verbeek, *Anal. Chim. Acta* **1967**, *37*, 332.
[43] M. Dusselier, P. Van Wouwe, A. Dewaele, E. Makshina, B. F. Sels, *Energy Environ. Sci.* **2013**, *6*, 1415.
[44] S. Han, D. Zhao, T. Otroshchenko, H. Lund, U. Bentrup, V. A. Kondratenko, N. Rockstroh, S. Bartling, D. E. Doronkin, J. D. Grunwaldt, U. Rodemerck, D. Linke, M. Gao, G. Jiang, E. V. Kondratenko, *ACS Catal.* **2020**, *10*, 8933.
[45] T. P. Araújo, J. Morales-Vidal, T. Zou, M. Agrachev, S. Verstraeten, P. O. Willi, R. N. Grass, G. Jeschke, S. Mitchell, N. López, J. Pérez-Ramírez, *Adv. Energy Mater.* **2023**, *13*, 2204122.
[46] J. Wang, G. Li, Z. Li, C. Tang, Z. Feng, H. An, H. Liu, T. Liu, C. Li, *Sci. Adv.* **2017**, *3*, e1701290.
[47] F. Yang, G. Li, P. Gao, X. N. Lv, X. Sun, Z. H. Liu, H. Fan, *Energy Technol.* **2013**, *1*, 581.
[48] See Supporting Information.
[49] J. P. Collman, K. M. Kosydar, M. Bressan, W. Lamanna, T. Garrett, *J. Am. Chem. Soc.* **1984**, *106*, 2569.
[50] J. Cao, Y. Lin, T. Zhou, W. Wang, Q. Zhang, B. Pan, W. Jiang, *iScience* **2023**, *26*, 107492.
[51] M. A. H. Alzuhairi, B. I. Khalil, R. S. Hadi, *Eng. Technol. J.* **2017**, *35*, 831.
[52] X. Cao, H. J. Lee, H. S. Yun, Y. M. Koo, *Korean J. Chem. Eng.* **2001**, *18*, 133.
[53] Z. B. Ke, X. H. Fan, D. You-Ying, F. Y. Che, L. J. Zhang, K. Yang, B. Li, Y. X. Kong, *Chem. Thermodyn. Therm. Anal.* **2022**, *5*, 100024.
[54] Y. Zhang, Y. Qi, Y. Yin, P. Sun, A. Li, Q. Zhang, W. Jiang, *ACS Sustainable Chem. Eng.* **2020**, *8*, 2865.
[55] H. Tsuji, in *Poly(Lactic Acid): Synthesis, Structures, Properties, Processing, and Applications* (Eds: R. A. Auras, L. T. Lim, S. E. M. Selke, H. Tsuji), Wiley, Hoboken **2010**.
[56] G. Gorrasi, R. Pantani, in *Synthesis, Structure and Properties of Poly(Lactic Acid)*. *Advances in Polymer Science* (Eds: M. D. Lorenzo, R. Androsch), Springer, Cham **2017**.
[57] E. T. H. Vink, K. R. Rábago, D. A. Glassner, B. Springs, R. P. O'Connor, J. Kolstad, P. R. Gruber, *Macromol. Biosci.* **2004**, *4*, 551.
[58] P. Coszach, J. C. Bogaert, J. Willocq, US 2012/0142958 A1, **2012**.
[59] M. S. Lehnertz, J. B. Mensah, R. Palkovits, *Green Chem.* **2022**, *24*, 3957.
[60] M. Qu, H. Tu, M. Amarante, Y. Q. Song, S. S. Zhu, *J. Appl. Polym. Sci.* **2014**, *131*, 40287.
[61] L. Pérez-Alvarez, E. Lizundia, L. Ruiz-Rubio, V. Benito, I. Moreno, J. L. Vilas-Vilela, *J. Appl. Polym. Sci.* **2019**, *136*, 47786.
[62] A. Moezzi, A. M. McDonagh, M. B. Cortie, *Chem. Eng. J.* **2012**, *185–186*, 1.
[63] A. Wang, W. Quan, H. Zhang, H. Li, S. Yang, *RSC Adv.* **2021**, *11*, 20465.
[64] F. Iannone, M. Casiello, A. Monopoli, P. Cotugno, M. C. Sportelli, R. A. Picca, N. Cioffi, M. M. Dell'Anna, A. Nacci, *J. Mol. Catal., A* **2017**, *426*, 107.
[65] M. Imran, D. H. Kim, W. A. Al-Masry, A. Mahmood, A. Hassan, S. Haider, S. M. Ramay, *Polym. Degrad. Stab.* **2013**, *98*, 904.
[66] J. T. Du, Q. Sun, X. F. Zeng, D. Wang, J. X. Wang, J. F. Chen, *Chem. Eng. Sci.* **2020**, *220*, 115642.
[67] M. Imran, K. G. Lee, Q. Imtiaz, B. K. Kim, M. Han, B. G. Cho, D. H. Kim, *J. Nanosci. Nanotechnol.* **2011**, *11*, 824.
[68] R. Wi, M. Imran, K. G. Lee, S. H. Yoon, B. G. Cho, D. H. Kim, *J. Nanosci. Nanotechnol.* **2011**, *11*, 6544.
[69] V. Vinitha, M. Preeyanghaa, M. Anbarasu, B. Neppolian, V. Sivamurugan, *Environ. Sci. Pollut. Res.* **2023**, *30*, 75401.
[70] M. Ehsani, K. Khodabakhshi, M. Asgari, *e-Polymers* **2014**, *14*, 353.
[71] L. Ramirez, M. L. Mecartney, S. P. Krumdieck, *J. Mater. Res.* **2008**, *23*, 2202.

[72] G. Štefanić, S. Musić, M. Ivanda, *J. Mol. Struct.* **2009**, *924–926*, 225.
[73] R. P. Ingel, D. Lewis, *J. Am. Ceram. Soc.* **1986**, *69*, 325.
[74] M. I. Zakirov, M. P. Semen'ko, O. A. Korotchenkov, *J. Nano-Electron. Phys.* **2018**, *10*, 05023.
[75] S. Tada, N. Ochiai, H. Kinoshita, M. Yoshida, N. Shimada, T. Joutsuka, M. Nishijima, T. Honma, N. Yamauchi, Y. Kobayashi, K. Iyoki, *ACS Catal.* **2022**, *12*, 7748.
[76] M. Kaniewski, M. Huculak-Maczka, J. Zieliński, M. Biegun, K. Hoffmann, J. Hoffmann, *Crystals* **2021**, *11*, 1250.
[77] P. N. Kuznetsov, L. I. Kuznetsova, A. M. Zhyzhaev, G. L. Pashkov, V. V. Bolyrev, *Appl. Catal. A* **2002**, *227*, 299.
[78] Y. Y. Tay, S. Li, C. Q. Sun, P. Chen, *Appl. Phys. Lett.* **2006**, *88*, 173118.
[79] N. Pauly, F. Yubero, J. P. Espinós, S. Tougaard, *Surf. Interface Anal.* **2019**, *51*, 353.
[80] W. Wang, H. T. Guo, J. P. Gao, X. H. Dong, Q. X. Qin. *J. Mater. Sci.* **2000**, *35*, 1495.
[81] E. A. Redekop, T. Cordero-Lanzac, D. Salusso, A. Pokle, S. Oien-Odegaard, M. F. Sunding, S. Diplas, C. Negri, E. Borfecchia, S. Bordiga, U. Olsbye, *Chem. Mater.* **2023**, *35*, 10434.
[82] M. T. Nikolajsen, J. C. Grivel, A. Gaur, L. P. Hansen, L. Baumgarten, N. C. Schjødt, U. V. Mentzel, J. D. Grunwaldt, J. Sehested, J. M. Christensen, M. Høj, *J. Catal.* **2024**, *431*, 115389.
[83] A. J. Martín, C. Mondelli, S. D. Jaydev, J. Pérez-Ramírez, *Chem* **2021**, *7*, 1487.
[84] K. V. Khopade, S. H. Chikkali, N. Barsu, *Cell Rep. Phys. Sci.* **2023**, *4*, 101341.
[85] M. Hestin, T. Faninger, L. Milios, in *Increased EU Plastics Recycling Targets: Environmental, Economic and Social Impact Assessment*, Plastic Recyclers Europe, Brussels, Belgium **2015**.